Combinatorial Source Inversion from Displacement and Tilt Measurements at Soufriere Hills Volcano Using a Self-Adapting Evolution Strategy

Joshua Taron

Department of Energy and Geo-Environmental Engineering
Pennsylvania State University
University Park, PA 16802

Abstract

A method is proposed to invert displacement and tilt measurements from a single monitoring location to constrain the nature of a volcanic pressure source. Evolutionary strategy is applied to a sequence of Mogi solutions and the program is shown capable of distinguishing between depth and volume increment of the magma source, in addition to its 3-dimensional spatial coordinates. The mechanism is applied to Soufriere Hills Volcano to constrain the nature of its single pressure source. Expansion to a two source scenario is also sought, but only one of the sources may be correctly constrained while the second is narrowed to several equally valid possibilities. The program is shown incapable of distinguishing between source pressure and radius for single or multiple sources.

1 INTRODUCTION

Deformation of the earth's crust surrounding volcanic episodes was first noticed by Japanese researchers in 1910, and was famously linked to predictable magnitudes via the expansion of a pressurized, point source in an infinite half space by Mogi (1958). Increases in monitoring capabilities around active volcanoes in more recent times have lead to the examination of well constrained geodetic influence on the nature and behavior of volcanic sources (Voight et al., 1998; Tiampo et al., 2000).

Many questions remain unanswered in attempts to ascertain the precise location of such a source. Conflicting values in the equations of crustal deformation when applied to inversion techniques limit researchers' ability to distinguish the values of individual parameters. The purpose of this work is to physically constrain the precise tendency of a volcanic source through the application of a self-adaptive evolution strategy.

2 THE EVOLUTIONARY ALGORITHM

In a contextual manner, evolutionary algorithms implement some formulation of three basic operators meant to mimic the process of biological evolution. The two primary sectors of evolutionary computation, evolution strategies (ES) (Rechenberg, 1965) and genetic algorithms (GA) (Holland, 1967), while devised independently, are of a similar theoretical nature and may be described in similar manner. Following the generation of a randomly distributed population of possible solutions over a feasible solution space, population members, or "parents", are evaluated with respect to an objective, or fitness, function. Next, the best solutions are: 1) selected in a manner that encourages 2) mating (recombination in ESs) of possible solutions, and some form of 3) mutation to inject diversity, or prevent the loss of alleles.

Evolutionary algorithms offer an attractive search strategy within complex search landscapes with multiple localized extrema, where traditional search methods such as conjugate gradients or linearized matrix inversion may fail. Creating the primary distinction between these and traditional methods is the ability to search a decision space from a full population of potential solutions. The ability of such random search methods to robustly locate global optima with general ease of implementation has increased their popularity in non-linear geophysical contexts and many other complex invocations.

Non-adaptive genetic algorithms have been previously applied to various geophysical inversion scenarios, such as to examine vertical seismic profiles (Horne and MacBeth, 1998), elastic-gravitational magma intrusion (Tiampo et al., 2004), surface displacement from magma intrusion (Tiampo et al., 2000), and geothermal magnetotelluric data (Perez-Flores and Schultz, 2002). Many variations of the evolutionary algorithm suffer the limitation that input problem variables may be quite specific to a given application, increasing the likelihood of false convergence if parameters are improperly tuned and the problem solution is not known beforehand. In such cases, it is often desirable to implement some form of adaptive parameter optimization, such as that presented by Reed *et al*., (2000). For this reason, it may be desirable to implement a form of self adaptive algorithm.

2.1 SELF ADAPTING EVOLUTION STRATEGY

Inversion in this work was conducted using the Covariance Matrix Adaptation Evolution Strategy (CMA-ES) (Hansen and Ostermeier, 2001). While randomized search algorithms are generally respected for their robustness in searching landscapes with multiple local optima and discontinuities, CMA-ES survives typical pitfalls of candidate evolution problems and, to a greater degree, overcomes badly scaled and non-separable problems through its self-learning strategy. Primary components of the learning strategy are the mean, *m*, or weighted average of optimum solutions in a given generation, the covariance matrix, C, and the mutation step size, σ.

New search points (offspring) are generated from a continuously adapting normal distribution. From this offspring population, λ, the best μ individuals are utilized in the solution vector to adjust the mean, m, of the normal distribution. By seeking an optimum covariance matrix of this normal distribution that approximates the inverse Hessian matrix, H^{-1}, the search distribution is adapted to follow the contour lines of the objective (fitness) function (see Hanson and Ostermeier (2001) for detailed analysis), thereby dictating the direction and size of the search space. Additional control is found via the step size parameter, σ, which is altered based upon the evolution path, or the evolution of population mean over several generations. In general, step size increases to allow a more diverse search region when optimal solutions are limiting, and decreases to funnel the search region when stronger convergence is desired, dictated by the evolution path.

Another strong benefit to CMA-ES is the lack of sensitivity to population size, which can plague population based search methods due to degeneration if the set value is not sufficiently high. Population degeneration in CMA-ES is avoided via the use of a learning rate in the adaptation of the covariance matrix. The primary benefits to CMA-ES, then, are: 1) Search distribution adaptation to accommodate severe landscapes, 2) population size insensitivity, and 3) prevention of premature convergence through step size control (Hansen and Ostermeier, 2001).

3 PRESSURE SOURCE MODEL

3.1 SURFACE DISPLACEMENT

The classical solution for deformation of the Earth's crust due to the activity of a pressurized magma source was presented by Anderson (1936) and, more famously, by Mogi (1958), for the geometry of a point source in an infinite half-space (Figure 1). That solution is,

$$u_z = \frac{a^3 \Delta P}{G} \frac{3d}{4\left(d^2 + r^2\right)^{3/2}}, \tag{1}$$

for vertical displacement, u_z, source depth, *d*, incremental pressure change (overpressure), ΔP, source radius, *a*, surface radial distance from the azimuth of the source to the monitoring location, *r*, and shear modulus, *G*, where the solution has utilized Lame's constant equal to 0.25 (thus issuing a poisson ratio of 0.25). The shear modulus may be expressed in familiar form for Young's modulus, *E*, and poisson ratio, υ, as $G = E/2(1+\upsilon)$. Displacements in the remaining spatial directions may be expressed in similar manner as,

$$u_x = \frac{a^3 \Delta P}{G} \frac{3x}{4\left(d^2 + r^2\right)^{3/2}} \tag{2}$$

$$u_y = \frac{a^3 \Delta P}{G} \frac{3y}{4\left(d^2 + r^2\right)^{3/2}}. \tag{3}$$

Limitations to the Mogi solution include the assumption of a small source radius in comparison to depth, thereby avoiding boundary influence from the half space for a non-infinite domain, and the existance of an infinite half-space of homogeneous medium. Contrary to this mathmatical limitation, the model has been applied with remarkable success to situations where the above constraint of depth to source radius does not hold (Dieterich and Decker, 1975; McTigue, 1987).

Characteristic of inversion scenarios, the Mogi solution, Eq. (1), in its capacity herein is subject to equifinality, or the tendency for multiple parameter combinations to produce valid global optimum. In other words, a deep source with large volume may produce the same surface deformation as a shallow source with small volume. As a result, distinguishing between *d*, *a*, ΔP, *x*, and *y* can prove to require necessary collaboration from additional data.

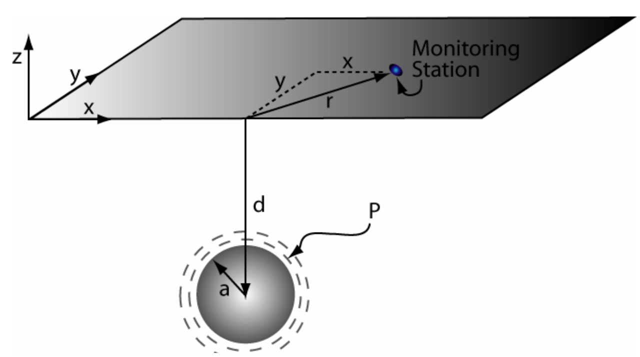

Figure 1: Geometry of a pressure source in an infinite half-space for depth, *d*, source radius, *a*, overpressure, *P*, and surface radial distance, *r*, to the point of measured deformation.

In an effort to better constrain parameters from the Mogi model, McTigue (1987) attempted to expand Eq. (1) to a higher order approximation. The expanded solution (derived in its entirety therein) is a sixth order approximation beyond the third order Mogi solution and represents the case of a finite cavity in half-space. None-the-less, McTigue (1987) observed the small effect of the addition and concluded that displacement was a poor indicator of source size, thus explaining the success of the Mogi solution at many depth ratios. Standard Mogi solutions may, therfore, be incapable of distinguishing between source radius and source pressure. An alternative formulation that bypasses the radius to pressure conflict and expresses, instead, these considations in terms of source volume change, ΔV, may be substituted into Eqs. (1)-(3) as (McTigue, 1987),

$$\Delta P a^3 = \frac{G \Delta V}{\pi}. \tag{4}$$

3.2 SURFACE RADIAL TILT

Source behavior may be further constrained by measurements of surface radial tilt, θ, expressed as the derivative of displacement,

$$\theta = \frac{9a^3 \Delta P}{4G} \frac{rd}{\left(r^2 + d^2\right)^{5/2}}, \tag{5}$$

which is, by definition, positive for an increase in magma source pressure or volume. Utilized herein is a combinatorial expression for the case where both tilt and deformation measurements are available. Interrelation of Eq. (1) and Eq. (5) yields,

$$\theta = \frac{3u_z d}{\left(r^2 + d^2\right)^{1/2}}. \tag{6}$$

4 OBJECTIVE FORMULATION

Evolutionary algorithms seek to maximize or minimize a given objective (fitness) function with respect to a desired outcome. When objective minimization is desirable, commonly referred to as a cost function, the algorithm will designate the global optimum at a user defined final fitness value. In this scenario, the objective is to minimize the difference between a measured geodetic value (time-series data) and one predicted by the above half-space models. This may be expressed as (Freund, 1979; Tiampo *et al.*, 2000),

$$F = \sum_{i=1}^{m} \frac{\left(\left(u_z, \theta\right)_i - f\left(x_i\right)\right)^2}{\sigma_i^2}, \tag{7}$$

for each measured value of displacement, u_{zi}, or tilt, θ_i, and its complementary predicted value for a set of trial solutions in the parent population, $f\left(x_i\right)$, normalized by the sample standard deviation, σ_i^2, of each time-series value from the mean of the time-series data set. The generalized purpose of the above relation is, therefore, to promote convergence of the CMA-ES/Mogi predictions, $f\left(x_i\right)$, to the mean of the time series data set.

With the above objective design, the five design variables include radius, a, depth, d, x distance, y distance, and overpressure, ΔP, for a single Mogi source model. This problem formulation will be expanded below to the examination of multiple source influence and a resulting 10 parameter fit.

5 MODEL VALIDATION

Internal model validation was sought via the generation of a synthetic subset of displacement and tilt values. A hypothetical pressure source was postulated, for values representative of Soufriere Hills Volcano, Montserrat, West Indies, at a depth of 1,000 m, x-distance of 620m, y-distance of 295m, radius of 200m, and supplanted to an overpressure of 4 MPa within a medium of shear modulus 0.6 GPa. The x and y coordinates correspond to monitoring location CP2 at Soufriere Hills (see Figure 1 of Widiwijayanti (2005)). These values were inserted into the sequence of Mogi equations to generate a synthetic time-series of tilt and displacement values. Synthetic data series were then disturbed by random Gaussian error representative of Montserrat monitoring locations, or $\pm$15mm displacement error and $\pm$10μrad tilt error (Figure 2). The model was then allowed to iterate on the five objective function parameters: x-distance, y-distance, depth, source radius, and pressure.

To include the impact of time-series dataset size on solution accuracy, the CMA-ES/Mogi program was set to loop along a monotonically increasing time series. At

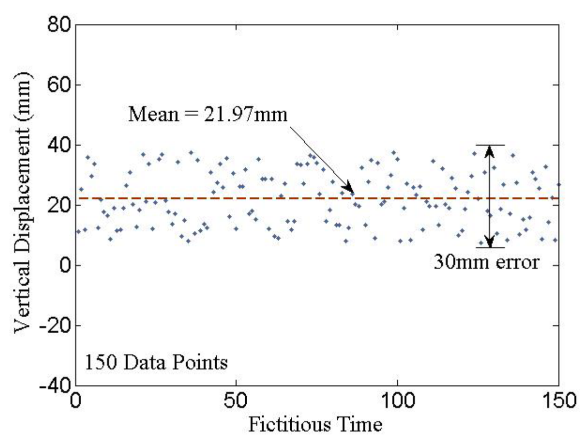

Figure 2: Sample of synthetic data series, shown here for vertical displacement with 150 generated fictitious points and $\pm$15mm Gaussian error. Values of dependent parameters are as stated in text.

Table 1: Average error in final values and number of required function evaluations for 50 random seed analysis with single Mogi source. All error values are in percent.

Data Set Size	x-Distance	y-Distance	Depth	Volume	# Fun. Evals.
20	0.601	1.498	0.291	1.770	709
40	0.354	0.518	0.297	0.738	1008
60	0.406	0.541	0.360	0.825	211
80	0.256	0.671	0.113	0.714	461
100	0.011	0.185	0.079	0.058	443

Table 2: Results from 50 random seed analysis for 2 monitoring locations with 100 member data sets.

Parameter	Average Error (%)
Source Volume	6.191
Monitoring Station 1	
x-Distance	3.315
y-Distance	9.339
Depth	2.658
Monitoring Station 2	
x-Distance	6.109
y-Distance	12.203
Depth	8.103

each value of dataset size, 50 random population seeds within CMA-ES were evaluated for final solution accuracy. The averaged 50 random seeds are presented in Table 1. From Table 1, the averaged trials converged to within 2% of the correct final value at all values of set size. Random seed effects were also present, such that the worst single seed experienced a final error of 12, 25, 35, and 40% for depth, x, y, and volume, respectively, at a set size of 100. This result highlights the importance of random seed analysis in any real world or trial application of EA's.

These results also show the ability of the Mogi combination presented herein to accurately differentiate between source depth and volume increment (pressure). The model cannot, however, recognize the separation between source radius and pressure, but instead must rely on the volume formulation of Eq. (4), which is predicted to within 2% of the correct value. To investigate the possible benefit of multiple data series in creating such a distinction, a separate model analysis was conducted by generating synthetic data series for two monitoring locations. The resulting evaluation incurred the additional parameters of x-distance, y-distance, and source depth for a second hypothetical monitoring location with added constraint from the full suite of Mogi relations. The second location was oriented at 471m, 249m, and 1000m in the x, y, and z directions, respectively, corresponding to monitoring station CP3 at Soufriere Hills (see Figure 1 of Widiwijayanti (2005)). However, while the final 8 parameter optimization was again nearly accurate for all location constraints, no added benefit was obtained with respect to a differentiation between source radius and pressure. Results of this analysis are shown in Table 2 for a single 50 random seed analysis. The synthetic time series were comprised of 100 data points.

6 MULTIPLE SOURCE FORMULATION

Also of interest is the ability of the algorithm to handle a larger array of uknown parameters. To examine this situation, a second pressure source was postulated at 400m, 700m, and 2500m in the x, y, and z directions, respectively, with a 100m radius and 6MPa pressure increment, while the first source maintained its specifications from the previous section. In a 50 random seed trial, with a set size of 200, 45 model runs resulted in a final error of less than 5% with respect to recreation of the original displacement and tilt values from the resulting optimized parameters, indicating accuracy in the final search. However, while 80% of the runs resulted in correct predicitons of all 5 parameters for the first source, a remarkably stable result, no distinct trend developed for favorability in prediction for the 5 parameters of the second source. Achieving accurate results in this scenario will, therefore, likely require the use of multiple time series.

7 APPLICATION TO SOUFRIERE HILLS

Following implementation of the CALPSO project on the island of Montserrat, West Indies, four monitoring boreholes were established in close proximity to the Soufriere Hills Volcano (SHV) in January 2003 (Linde et al., 2005). From these monitoring locations, a full suite of deformation and tilt time series allow a detailed analysis of source characteristics through the mechanism outlined herein. Previous studies (Linde *et al.*, 2005; Widiwijayanti *et al.*, 2005) have postulated the existence of a Mogi like source beneath SHV, leading to possible representation via the single source model validated above.

Displacement and tilt records were collected from the SHV monitoring location at 16.741 N and 297.832 E. Variability in the records is approximately $\pm$15mm for displacement and $\pm$10μrad for tilt. Utilizing a time series with 50 data points, an analysis of 100 random seeds was conducted. Progression of parameter values is followed in FIGURE for a single seed analysis, where the final values approach 576m, 302m, and 982m in the x, y, and z directions, with volume increment, as a function of

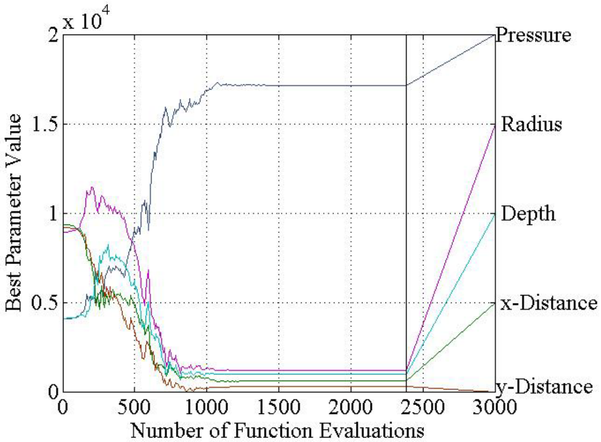

Figure 3: Parameter value evolution for CMA-ES/Mogi analysis of single pressure source for Soufriere Hills. Spatial parameters converge to their correct values, while strong variability is present for pressure and radius. Volume increment (a function solely of radius and pressure) is, however, very stable for all seed analyses.

pressure and radius, of 1.32×10^{-4} km^3. The 100 random seed analysis resulted in 100% convergence of all final values to within a 5% grouping. Applying the error values obtained in the validation section of 2% for a 50 seed analysis, results in a $\pm$20m variability in final distance results.

8 CONCLUSION

Sequencing four incantations of the Mogi source equations with CMA-ES resulted in a successful one-source validation for the prediction of spatial location and volume increment for a magmatic source in a homogeneous and infinite elastic half-space. Expanding this to the case when multiple time-series are available from multiple monitoring locations resulted in no added benefit, as the Mogi solutions are unable to distinguish between source pressure and radius. A multiple source scenario showed effective prediction of one of the sources, but strong variability in parameters of the second source. Even in this case, however, the CMA-ES/Mogi coupling showed a high percentage of convergence to a correct combination of parameters to generate the input displacement and tilt. Variability in this sense is, then, only a function of the strong equifinality of the inversion.

REFERENCES

Anderson, E. M. (1936). Dynamics of the formation of cone-sheets, ring-dykes, and cauldron-subsidences. *Proceedings of the Royal Society of Edinburgh* 56: 128-157.

Dieterich, J. H. and R. W. Decker (1975). Finite element modeling of surface deformation associated with volcanism. *Journal of Geophysical Research* 90(11): 11,199-11,209.

Freund, J. E. (1979). Modern elementary statistics, Fifth Edition. Prentice-Hall International, Inc., London, 510 pp.

Hansen, N. and A. Ostermeier (2001). Completely Derandomized Self-Adaptation in Evolution Strategies. *Evolutionary Computation* 9(2): 159-195.

Holland, J. H. (1967). Nonlinear environments permitting efficient adaptation. *Computer and Information Sciences II (New York: Academic)*.

Horne, S. and C. MacBeth (1998). A comparison of global optimisation methods for near-offset VSP inversion. *Computers & Geosciences* 24(6): 563-572.

Linde, A., S. Sacks, et al. (2005). The explosion of March 2004 at Montserrat: constraints from borehole strain data. In Eos Transactions AGU, 86(52), Fall Meet. Suppl., Abstract V53B-1571.

McTigue, D. F. (1987). Elastic stress and deformation near a finite spherical magma body: resolution of the point source paradox. *Journal of Geophysical Research* 92(B12): 12,931-12,940.

Mogi, K. (1958). Relations between the eruptions of various volcanoes and the deformations of the ground surfaces around them. *Bulletin of the Earthquake Research Institute of Tokyo* 36: 99-134.

Perez-Flores, M. A. and A. Schultz (2002). Application of 2-D inversion with genetic algorithms to magnetotelluric data from geothermal areas. *Earth Planets Space* 54: 607-616.

Rechenberg, I. (1965). Cybernetic solution path of an experimental problem. *Royal Aircraft Establishment Library Translation 1122*.

Reed, P., B. Minsker, et al. (2000). Designing a competent simple genetic algorithm for search and optimization. *Water Resources Research* 36(12): 3757-3761.

Tiampo, K. F., J. Fernandez, et al. (2004). Volcanic source inversion using a genetic algorithm and an elastic-gravitational layered earth model for magmatic intrusions. *Computers & Geosciences* 30(9-10): 985-1001.

Tiampo, K. F., J. B. Rundle, et al. (2000). Spherical and ellipsoidal volcanic sources at Long Valley caldera, California, using a genetic algorithm inversion technique.

Journal of Volcanology and Geothermal Research 102(3-4): 189-206.

Voight, B., R. P. Hoblitt, et al. (1998). Remarkable cyclic ground deformation monitored in real-time on Montserrat, and its use in eruption forcasting. *Geophysical Research Letters* 25: 3405-3408.

Widiwijayanti, C., A. Clarke, et al. (2005). Geodetic constraints on the shallow magma system at Soufriere Hills Volcano, Montserrat. *Geophysical Research Letters* 32.